Am J Physiol Heart Circ Physiol 288: H1820–H1828, 2005.
First published December 2, 2004; doi:10.1152/ajpheart.00589.2004.

Mitochondrial membrane potential modulates regulation of mitochondrial Ca^{2+} in rat ventricular myocytes

Masao Saotome, Hideki Katoh, Hiroshi Satoh, Shiro Nagasaka, Shu Yoshihara, Hajime Terada, and Hideharu Hayashi

Third Department of Internal Medicine, Hamamatsu University School of Medicine, Hamamatsu, Japan

Submitted 15 June 2004; accepted in final form 18 November 2004

Saotome, Masao, Hideki Katoh, Hiroshi Satoh, Shiro Nagasaka, Shu Yoshihara, Hajime Terada, and Hideharu Hayashi. Mitochondrial membrane potential modulates regulation of mitochondrial Ca^{2+} in rat ventricular myocytes. *Am J Physiol Heart Circ Physiol* 288: H1820–H1828, 2005. First published December 2, 2004; doi:10.1152/ajpheart.00589.2004.—Although recent studies focused on the contribution of mitochondrial Ca^{2+} to the mechanisms of ischemia-reperfusion injury, the regulation of mitochondrial Ca^{2+} under pathophysiological conditions remains largely unclear. By using saponin-permeabilized rat myocytes, we measured mitochondrial membrane potential ($\Delta\Psi_m$) and mitochondrial Ca^{2+} concentration ($[Ca^{2+}]_m$) at the physiological range of cytosolic Ca^{2+} concentration ($[Ca^{2+}]_c$; 300 nM) and investigated the regulation of $[Ca^{2+}]_m$ during both normal and dissipated $\Delta\Psi_m$. When $\Delta\Psi_m$ was partially depolarized by carbonyl cyanide *p*-(trifluoromethoxy)phenylhydrazone (FCCP, 0.01–0.1 μM), there were dose-dependent decreases in $[Ca^{2+}]_m$. When complete $\Delta\Psi_m$ dissipation was achieved by FCCP (0.3–1 μM), $[Ca^{2+}]_m$ remained at one-half of the control level despite no Ca^{2+} influx via the Ca^{2+} uniporter. The $\Delta\Psi_m$ dissipation by FCCP accelerated calcein leakage from mitochondria in a cyclosporin A (CsA)-sensitive manner, which indicates that $\Delta\Psi_m$ dissipation opened the mitochondrial permeability transition pore (mPTP). After FCCP addition, inhibition of the mPTP by CsA caused further $[Ca^{2+}]_m$ reduction; however, inhibition of mitochondrial Na^+/Ca^{2+} exchange (mitoNCX) by a Na^+-free solution abolished this $[Ca^{2+}]_m$ reduction. Cytosolic Na^+ concentrations that yielded one-half maximal activity levels for mitoNCX were 3.6 mM at normal $\Delta\Psi_m$ and 7.6 mM at $\Delta\Psi_m$ dissipation. We conclude that *1*) the mitochondrial Ca^{2+} uniporter accumulates Ca^{2+} in a manner that is dependent on $\Delta\Psi_m$ at the physiological range of $[Ca^{2+}]_c$; *2*) $\Delta\Psi_m$ dissipation opens the mPTP and results in Ca^{2+} influx to mitochondria; and *3*) although mitoNCX activity is impaired, mitoNCX extrudes Ca^{2+} from the matrix even after $\Delta\Psi_m$ dissipation.

permeability transition pore; Na^+/Ca^{2+} exchange; depolarization; ischemia-reperfusion injury

ACCUMULATING EVIDENCE REVEALS that mitochondria play primary roles in fatal cell damage during ischemia-reperfusion (33). Key events that occur during ischemia include cytosolic Ca^{2+} elevation, ATP depletion, high P_i concentration, depolarized membrane potential, and acidotic pH. On reperfusion and recovery of normal pH, a burst of reactive oxygen species occurs, mitochondrial Ca^{2+} overload ensues, and these lead to opening of the mitochondrial permeability transition pore (mPTP; Refs. 8, 12, 34). Opening of the mPTP allows water and solutes ≤1,500 Da in size to enter the matrix and cause mitochondrial swelling, rupture of the outer mitochondrial membrane, and release of cytochrome *c* or apoptosis-inducing factor, which initiates apoptotic programmed cell death (12, 24, 34). Because previous studies (8, 12, 13) have shown that the opening of the mPTP is largely dependent on mitochondrial Ca^{2+}, it is important to understand the properties of the regulatory systems for mitochondrial Ca^{2+} concentration ($[Ca^{2+}]_m$) during pathophysiological conditions such as ischemia and reperfusion.

Under normal conditions, the mitochondrial inner membrane remains impermeable to ions and possesses several Ca^{2+} transport systems for the regulation of $[Ca^{2+}]_m$ (4, 6, 10, 11). Ca^{2+} accumulation into mitochondria occurs via the Ca^{2+} uniporter, which is driven by the negative charge of the mitochondrial membrane potential ($\Delta\Psi_m$). The Ca^{2+} uniporter is activated by extra-mitochondrial Ca^{2+}, ADP, and spermine and is inhibited by Mg^{2+} and ruthenium red (RuR; Refs. 10, 11). Extrusion of mitochondrial Ca^{2+} is mediated primarily via mitochondrial Na^+/Ca^{2+} exchange (mitoNCX) in cardiac myocytes. The mitoNCX is activated by nigericin and the pH or Na^+ gradients between the matrix and the cytosol and is inhibited by diltiazem, clonazepam, CGP-37157, and Mg^{2+} (6, 10, 11). For another Ca^{2+} efflux pathway, mitochondria have the slow, relatively small Ca^{2+}/H^+ exchange, which is not dominant in cardiac tissues (10, 11). Furthermore, recent studies (4, 8, 10, 11, 18) also suggest a possible contribution by the mPTP to Ca^{2+} homeostasis in both the cytosol and mitochondria.

Despite the considerable attention given to the pathophysiological significance of mitochondrial Ca^{2+}, the regulation and/or modulation of mitochondrial Ca^{2+} during pathophysiological conditions such as ischemia-reperfusion injury are unclear. In previous studies, information about mitochondrial Ca^{2+} was obtained using isolated mitochondria, whereby the structural and functional properties of organelles were seriously affected, and other cellular architectures were separated from the mitochondria. In this study, we measured $[Ca^{2+}]_m$ in saponin-permeabilized rat ventricular myocytes and investigated how $\Delta\Psi_m$ depolarization affects $[Ca^{2+}]_m$ and mitochondrial Ca^{2+} transport systems such as the Ca^{2+} uniporter, the mPTP, and mitoNCX.

MATERIALS AND METHODS

Cell isolation and solutions. This investigation is in conformance with the *Guide for the Care and Use of Laboratory Animals* published by the National Institutes of Health (NIH Publication No. 85-23, revised 1996). Isolated myocytes were obtained from male Sprague-Dawley rats (body wt, 250–300 g) by enzymatic dissociation, and the

Address for reprint requests and other correspondence: H. Katoh, Division of Cardiology, Internal Medicine III, Hamamatsu Univ. School of Medicine, 1-20-1 Handayama, Hamamatsu 431-3192, Japan (E-mail: hkatoh@hama-med.ac.jp).

The costs of publication of this article were defrayed in part by the payment of page charges. The article must therefore be hereby marked "*advertisement*" in accordance with 18 U.S.C. Section 1734 solely to indicate this fact.

0363-6135/05 $8.00 Copyright © 2005 the American Physiological Society

Downloaded from http://ajpheart.physiology.org/ by 10.220.33.5 on October 6, 2016

cells were kept in a modified Kraftbrühe solution (15, 29) that contained (in mM) 70 KOH, 40 KCl, 20 KH_2PO_4, 3 $MgCl_2$, 50 glutamic acid, 10 glucose, 10 HEPES, and 0.5 EGTA (pH 7.4 with KOH). Just before the experiment, cells were placed in a chamber and perfused with a normal Tyrode solution composed of (in mM) 143 NaCl, 5.4 KCl, 0.5 $MgCl_2$, 0.25 NaH_2PO_4, 1 $CaCl_2$, 5.6 glucose, and 5 HEPES (pH 7.4 with NaOH). All experiments were conducted at room temperature (22°C) within 6 h of cell isolation.

Measurement of $[Ca^{2+}]_m$ in skinned myocytes. Isolated rat ventricular myocytes were loaded with 20 μM rhod-2-AM at room temperature for 60 min. To remove cytosolic rhod-2, the sarcolemmal membrane was permeabilized by perfusion of saponin (0.05 mg/ml) in a Ca^{2+}-free internal solution that contained (in mM) 50 KCl, 80 potassium aspartate, 4 sodium pyruvate, 20 HEPES, $3MgCl_2 \cdot 6H_2O$, 3 Na_2ATP, 5.8 glucose, and 3 EGTA (pH 7.3 with KOH). After the sarcolemmal membrane was permeabilized, the free Ca^{2+} concentration in the internal solution ($[Ca^{2+}]_c$) was increased according to the experimental protocol. The $[Ca^{2+}]_c$ was obtained by mixture of EGTA and $CaCl_2$ and was calculated using the WIN MAXC 2.1 computer program (provided by Stanford University).

Experiments were performed using a laser-scanning confocal microscope (LSM 510; Zeiss) coupled to an inverted microscope (Axiovert S100; Zeiss) with a ×63 water-immersion objective lens (numerical aperture, 1.3). Cells were excited with the 514-nm-wavelength argon laser, and images were acquired through a >560-nm long-pass filter. For quantitative analysis of the changes in rhod-2 signals, fluorescence intensities at identical regions of interest (20 × 20 pixels) were monitored every 30 or 60 s.

To localize mitochondria, some myocytes were coloaded with rhod-2-AM and Mito Tracker Green (excitation wavelength, 488 nm; emission wavelength, through a 505–530-nm band-pass filter). RuR (1 μM), which is an inhibitor of the mitochondrial Ca^{2+} uniporter, or FCCP (0.0–1 μM), which is an uncoupler of the mitochondrial respiratory chain, was used to modify $[Ca^{2+}]_m$.

Measurement of $\Delta\Psi_m$. For $\Delta\Psi_m$ measurement, cells were initially permeabilized and loaded using a continuous perfusion of the fluorescent indicator tetramethylrhodamine ethyl ester (TMRE; 20 nM). TMRE was excited at a 543-nm wavelength with a helium-neon laser, and the emission signals were collected through a 580-nm long-pass filter. For the steady measurements of time-dependent fluorescence changes, images were recorded after 20 min of TMRE perfusion.

Imaging of mPTP opening. To evaluate mPTP opening, myocytes were loaded with calcein-AM (1 μM) for 15 min, and the sarcolemmal membrane was permeabilized to remove cytoplasmic dyes. This method allows for selective loading of calcein in mitochondria. On the opening of the mPTP, entrapped calcein is released from the mito-

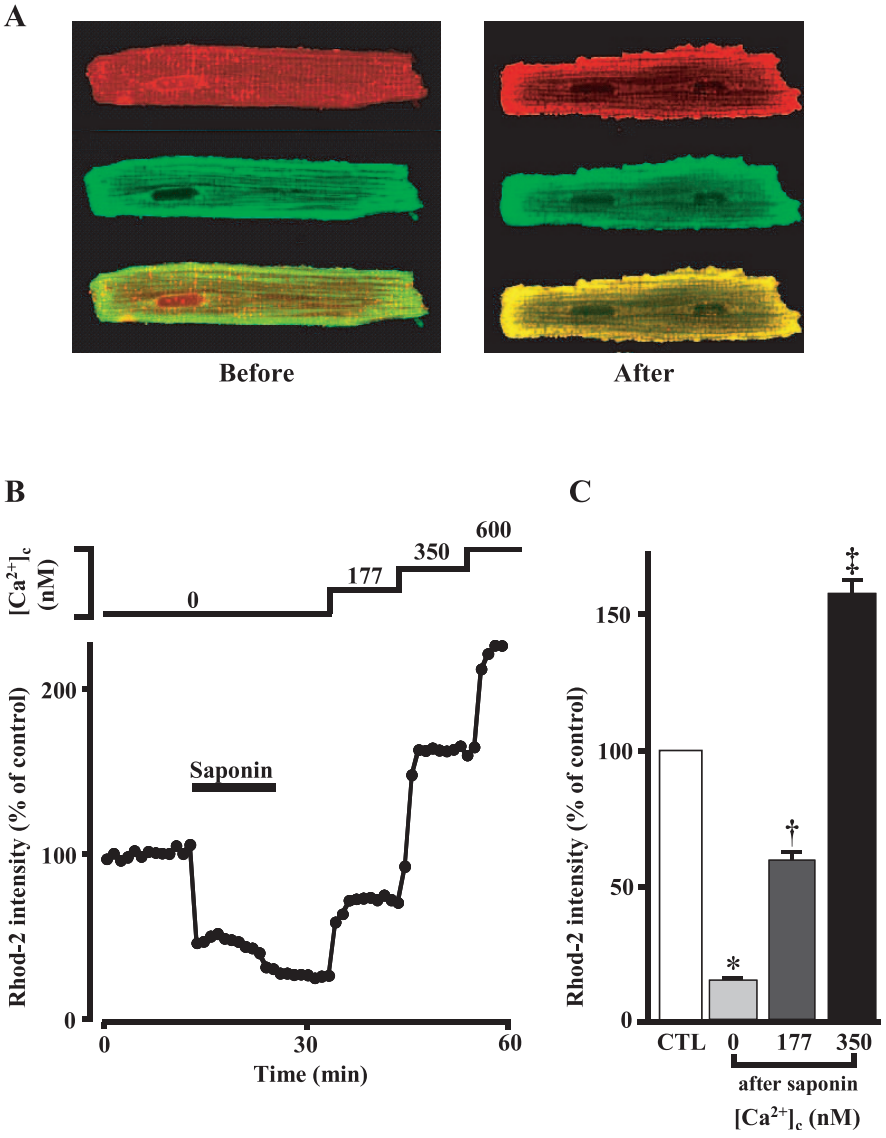

Fig. 1. Measurement of mitochondrial Ca^{2+} concentration ($[Ca^{2+}]_m$) with rhod-2-AM in permeabilized myocytes. *A*: confocal images of rhod-2 (*top*; red), Mito Tracker Green (*middle*; green), and their superimposition (*bottom*) in a single myocyte. Images were obtained before and after permeabilization of sarcolemmal membrane. *B*: a representative recording of the changes in rhod-2 signal in a single myocyte. After sarcolemmal membrane was permeabilized, the Ca^{2+} concentration of the internal solution ($[Ca^{2+}]_c$) was increased as indicated (*top*). *C*: summarized data of the rhod-2 signals before and after membrane permeabilization. Data are presented as the percentage of control (CTL; 0 Ca^{2+} before saponin). Values are means ± SE; $n = 4$; *$P < 0.01$ vs. control; †$P < 0.01$ vs. 0 Ca^{2+}; and ‡$P < 0.01$ vs. 177 nM Ca^{2+} by paired *t*-test.

Downloaded from http://ajpheart.physiology.org/ by 10.220.33.5 on October 6, 2016

chondrial matrix (20, 30). Calcein was excited at a 488-nm wavelength, and emission was collected through a 505- to 550-nm bandpass filter.

Chemicals and data analysis. All chemicals were obtained from Sigma (St. Louis, MO), and fluorescent dyes were purchased from Molecular Probes (Eugene, OR). Data are presented as means ± SE; *n* describes the number of cells or experiments. Statistical analyses were performed using *t*-test or ANOVA. A level of $P < 0.05$ was accepted as statistically significant.

RESULTS

Determination of $[Ca^{2+}]_m$. We first compared the rhod-2 signals before and after permeabilization of the sarcolemmal membrane in the rhod-2-AM-loaded myocytes to determine the fraction of fluorescence signals that originated from the mitochondria. Figure 1*A* demonstrates the dual-stained images of rhod-2 and Mito Tracker Green (which was used to identify the localization of mitochondria). As shown in Fig. 1*A* (*left*), the distributions of rhod-2 (*top*) and Mito Tracker Green (*middle*) were not identical before the permeabilization, and there were red areas that were loaded only by rhod-2 in the superimposed image (*bottom*). However, after the sarcolemmal membrane was permeabilized in the same cell (Fig. 1*A*, *right*), both fluorescent indicators overlapped almost completely (yellow in the superimposed image). These results indicate that when cells are loaded with rhod-2-AM, some amount of dye remains in the cytosolic space, and this dye was released after the permeabilization. As shown in Fig. 1*B*, the rhod-2 signal decreased rapidly after membrane permeabilization and increased in response to incremental $[Ca^{2+}]_c$ changes to 177, 350, and 600 nM. Summarized data in Fig. 1*C* demonstrate that after membrane permeabilization, the rhod-2 signal decreased to 15 ± 1% of its intensity before permeabilization ($P < 0.01$; $n = 4$), and the incremental $[Ca^{2+}]_c$ changes increased the rhod-2 signal to 60 ± 5% ($[Ca^{2+}]_c = 177$ nM; $P < 0.01$ vs. 0 Ca^{2+} after saponin) and 159 ± 7% ($[Ca^{2+}]_c = 350$ nM; $P < 0.01$ vs. $[Ca^{2+}]_c = 177$ nM) of the control value (before saponin), respectively.

To confirm that the changes of rhod-2 signals in permeabilized myocytes indeed reflect $[Ca^{2+}]_m$, we examined the effects of mitochondrial Ca^{2+} uniporter inhibition by RuR, which is an inhibitor of the Ca^{2+} uniporter. As shown in Fig. 2*A*, repeated exposure to the 300 nM $[Ca^{2+}]_c$ (without drugs)

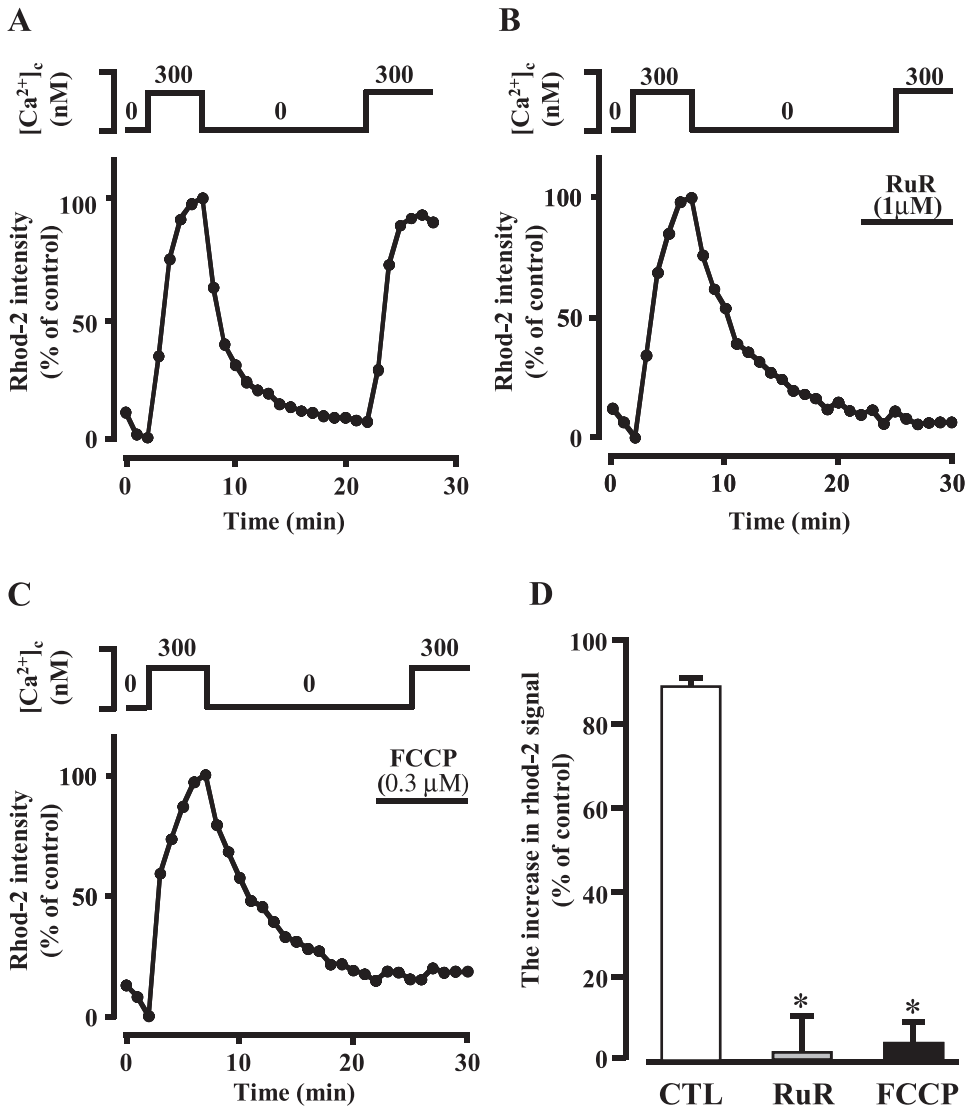

Fig. 2. Effects of mitochondrial Ca^{2+} uniporter inhibition on the rhod-2 signal in permeabilized myocytes. *A–C*: representative recordings of rhod-2 signals in permeabilized myocytes. *A*: a myocyte was exposed to $[Ca^{2+}]_c$ of 300 nM for 5 min, and after a 15-min perfusion with Ca^{2+}-free solution, $[Ca^{2+}]_c$ was elevated to 300 nM again (*top*). *B* and *C*: before the second addition of Ca^{2+}, myocytes were pretreated with 1 μM ruthenium red (RuR, to inhibit the Ca^{2+} uniporter; *B*) or 0.3 μM carbonyl cyanide *p*-(trifluoromethoxy)phenylhydrazone (FCCP, to eliminate the driving force of the Ca^{2+} uniporter; *C*) for 3 min, and then Ca^{2+} was add to the internal solution. *D*: summarized data of the increases in rhod-2 intensities after the second addition of Ca^{2+} without drugs (control, $n = 4$), with RuR ($n = 5$), and with FCCP ($n = 5$). Rhod-2 signals in the first 300 nM Ca^{2+} were referred to as control, and data are presented as percentages of control. *$P <$ 0.01 vs. control by nonpaired *t*-test.

Downloaded from http://ajpheart.physiology.org/ by 10.220.33.5 on October 6, 2016

caused rapid increases in the rhod-2 signal, whereas in the cells pretreated with 1 μM RuR, the rhod-2 signal increase was completely inhibited even in 300 nM $[Ca^{2+}]_c$ (Fig. 2*B*). The inhibitory effects of the Ca^{2+} uniporter on the rhod-2 signal were further verified by treating cells with 0.3 μM FCCP, which is a respiratory chain uncoupler that abolishes the driving force for the Ca^{2+} uniporter via $\Delta\Psi_m$ depolarization. FCCP was applied to the Ca^{2+}-free solution, and $[Ca^{2+}]_c$ was increased to 300 nM in the presence of FCCP. FCCP pretreatment also inhibited the rhod-2 signal increase that was caused by addition of 300 nM Ca^{2+} (Fig. 2*C*). Summarized data in Fig. 2*D* show that rhod-2 intensities in the permeabilized myocytes increased by the second addition of 300 nM Ca^{2+} (control, 88 ± 2% of the first 300 nM Ca^{2+}; $n = 4$), and that pretreatment with RuR (2 ± 9%; $P < 0.01$ vs. control, $n = 5$) or FCCP (4 ± 5%; $P < 0.01$ vs. control; $n = 5$) abolished the increase in the rhod-2 signal. These results indicate that *1*) Ca^{2+} influx into mitochondria is mainly mediated via the Ca^{2+} uniporter, *2*) the driving force for the Ca^{2+} uniporter largely depends on $\Delta\Psi_m$, and *3*) there is no net mitochondrial Ca^{2+} uptake via the Ca^{2+} uniporter during conditions of $\Delta\Psi_m$ dissipation.

Because the rhod-2 signal in permeabilized myocytes increased in response to the change in $[Ca^{2+}]_c$, and this rhod-2 signal increase was abolished by inhibition of the mitochondrial Ca^{2+} uniporter (by RuR or FCCP), we confirmed that rhod-2 signals in the permeabilized myocytes represent $[Ca^{2+}]_m$.

Effects of $\Delta\Psi_m$ on $[Ca^{2+}]_m$. In this series of experiments, we investigated the effects of $\Delta\Psi_m$ depolarization on $[Ca^{2+}]_m$ in permeabilized myocytes. Figure 3*A* shows a representative recording of TMRE intensity (which represents $\Delta\Psi_m$) after application of FCCP to the internal solution ($[Ca^{2+}]_c = 300$ nM). Lower concentrations of FCCP (0.01–0.1 μM) depolarized $\Delta\Psi_m$ in a dose-dependent manner, whereas 1 μM FCCP dissipated $\Delta\Psi_m$ completely. Figure 3*B* shows a typical recording of rhod-2 intensity after application of FCCP to 300 nM $[Ca^{2+}]_c$. Lower concentrations of FCCP (0.01–0.1 μM) dose dependently decreased $[Ca^{2+}]_m$, whereas $[Ca^{2+}]_m$ remained at almost one-half of the control level even after application of 1 μM FCCP. Figure 3*C* shows that when $\Delta\Psi_m$ was partially depolarized by lower concentrations of FCCP [0.01 μM: 83 ± 2% of value before FCCP administration (control); $P < 0.01$ vs. control; $n = 4$; and 0.1 μM: 37 ± 4%; $P < 0.01$ vs. 0.01 μM FCCP; $n = 13$], there were corresponding reductions in $[Ca^{2+}]_m$ [0.01 μM: 85 ± 5% of value before FCCP administration (control); $P < 0.05$ vs. control; $n = 4$; and 0.1 μM: 67 ± 6%; $P < 0.01$ vs. 0.01 μM FCCP; $n = 7$]. However, under conditions of complete $\Delta\Psi_m$ dissipation by 0.3 or 1 μM FCCP (which means no driving force for the Ca^{2+} uniporter), the reductions in $[Ca^{2+}]_m$ were incomplete, and $[Ca^{2+}]_m$ remained at 53 ± 1% (0.3 μM; $n = 4$) and 55 ± 4% (1 μM; $n = 6$) of the control value, respectively. Because FCCP might alter the properties of mitochondrial Ca^{2+} transport systems through changes in matrix pH, we also tested the effects of the K^+ ionophore valinomycin on $\Delta\Psi_m$ and $[Ca^{2+}]_m$. When the application of 10 nM valinomycin dissipated $\Delta\Psi_m$, the decrease of $[Ca^{2+}]_m$ also remained at one-half of the control level (data not shown). These results suggest that when FCCP is applied, changes in matrix pH might not be responsible for the changes in the mitochondrial Ca^{2+} transport systems. Because the mitochondrial Ca^{2+} influx is mainly mediated via the Ca^{2+} uniporter, and the driving force for the Ca^{2+} uniporter depends on $\Delta\Psi_m$, these results suggest that *1*) mitochondrial Ca^{2+} influx via the Ca^{2+} uniporter decreased when $\Delta\Psi_m$ was partially depolarized, and *2*) Ca^{2+}-regulating pathways other than the Ca^{2+} uniporter were involved when $\Delta\Psi_m$ was completely dissipated.

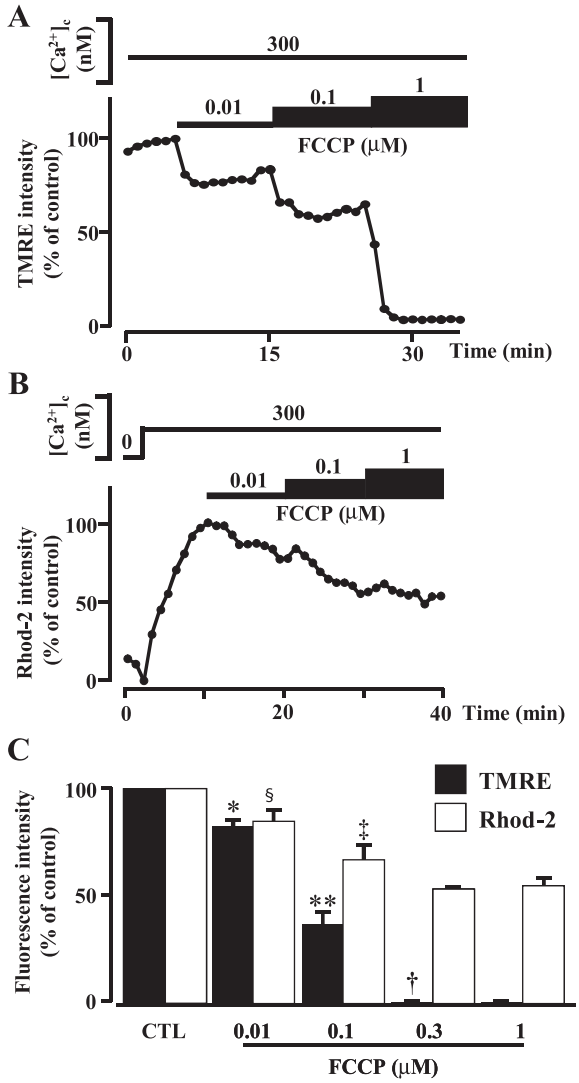

Fig. 3. Effects of FCCP on the changes in mitochondrial membrane potential ($\Delta\Psi_m$) and $[Ca^{2+}]_m$. *A* and *B*: representative recordings of tetramethylrhodamine ethyl ester (TMRE; *A*) and rhod-2 (*B*) signals after application of FCCP ($[Ca^{2+}]_c = 300$ nM) in permeabilized myocytes. FCCP was applied as shown (*A* and *B*, *top*). Data are expressed as the percentage of value before FCCP application (control). *C*: summarized data from 4 to 13 experiments. *$P < 0.01$ vs. control (TMRE signal before FCCP administration); **$P < 0.01$ vs. TMRE with 0.01 μM FCCP; †$P < 0.01$ vs. TMRE with 0.1 μM FCCP; §$P < 0.05$ vs. control (rhod-2 signal before FCCP administration); ‡$P < 0.01$ vs. rhod-2 with 0.01 μM FCCP by nonpaired *t*-test.

Imaging of mPTP opening by calcein. Because it has been reported that the mPTP serves as a mitochondrial Ca^{2+} flux pathway, and depolarization of $\Delta\Psi_m$ renders the mPTP to be opened (5, 22, 23), we hypothesized that the mPTP could contribute to the regulation of $[Ca^{2+}]_m$ in the situation of $\Delta\Psi_m$ dissipation. Therefore, in this series of experiments, we investigated whether $\Delta\Psi_m$ dissipation by FCCP induces mPTP

Downloaded from http://ajpheart.physiology.org/ by 10.220.33.5 on October 6, 2016

opening by measuring calcein leakage from the mitochondria. The confocal images in Fig. 4*A* show that calcein fluorescence in a permeabilized myocyte decreased after 15 min of FCCP perfusion (0.3 μM). In contrast, when cells were pretreated with the mPTP inhibitor cyclosporine A (CsA; 0.1 μM), the reduction in the calcein signal by FCCP was notably inhibited (Fig. 4*B*). Figure 4*C* shows the time courses of the changes in calcein signals after perfusion of a control solution ($[Ca^{2+}]_c$ = 300 nM), CsA (0.1 μM), FCCP (0.3 μM), and FCCP plus CsA, and Fig. 4*D* summarizes the calcein intensities after a 15-min perfusion of each solution. The application of FCCP significantly decreased the calcein signal to 83 ± 3% of the baseline level (FCCP, $P < 0.01$ vs. 95 ± 1% of control; $n = 5$), whereas the decrease in the calcein signal by FCCP was inhibited in the presence of CsA (FCCP plus CsA, 93 ± 1%; $P < 0.01$ vs. FCCP; $n = 5$). These results suggest that $\Delta\Psi_m$ dissipation by FCCP opened the mPTP in a CsA-sensitive manner.

Contribution of mPTP opening to $[Ca^{2+}]_m$. To investigate whether there is an mPTP-related mitochondrial Ca^{2+} flux, we examined the effects of CsA on the changes in $[Ca^{2+}]_m$ when $\Delta\Psi_m$ was dissipated by FCCP. As shown in Fig. 5*A*, in the cells pretreated with 0.1 μM CsA, the rhod-2 signal after perfusion of 0.3 μM FCCP decreased more than that of FCCP alone. When the mPTP was inhibited by pretreatment with CsA, the rhod-2 signal after a 15-min FCCP perfusion was 25 ± 6% of the level before FCCP perfusion ($P < 0.01$; 53 ± 1% of FCCP alone; $n = 4$), which indicates that there was a CsA-sensitive decrease in $[Ca^{2+}]_m$. These results suggest that mPTP inhibition reduces Ca^{2+} influx into the mitochondria during conditions of $\Delta\Psi_m$ dissipation.

Ca^{2+} efflux via mitoNCX when $\Delta\Psi_m$ is dissipated. Next we focused on the properties of mitochondrial Ca^{2+} efflux after $\Delta\Psi_m$ dissipation. Because previous studies using isolated mitochondria indicated that mitoNCX is a main Ca^{2+} efflux pathway in cardiac myocytes (6, 32), we examined the effects of mitoNCX inhibition on $[Ca^{2+}]_m$ under conditions of dissipated $\Delta\Psi_m$. Figure 5*B* shows the changes in $[Ca^{2+}]_m$ after FCCP perfusion (0.3 μM) in a normal-Na^+ {extra-mitochondrial Na^+ concentration ($[Na^+]_c$), 10 mM} or a Na^+-free ($[Na^+]_c$, 0 mM) internal solution. To eliminate the effects of mPTP-related Ca^{2+} flux, myocytes were pretreated with 0.1 μM CsA. When cells were perfused with FCCP, $[Ca^{2+}]_m$ declined rapidly in the normal-Na^+ solution, whereas $[Ca^{2+}]_m$ did not decrease in the Na^+-free solution. When mitoNCX was inhibited by a Na^+-free solution, the rhod-2 signal after a 15-min FCCP perfusion was 84 ± 8% compared with before FCCP perfusion ($[Na^+]_c$ = 0 mM: $P < 0.01$ vs. 25 ± 6% of $[Na^+]_c$ = 10 mM; $n = 4$), which indicates that the extrusion of mitochondrial Ca^{2+} was almost abolished. These results suggest that even after complete $\Delta\Psi_m$ dissipation, mitoNCX extrudes Ca^{2+} from mitochondria.

Finally, we investigated the effects of $[Na^+]_c$ on the rates of Ca^{2+} extrusion by mitoNCX in both normal and dissipated $\Delta\Psi_m$. In this series of experiments, to exclude the contribution of Ca^{2+} influx into mitochondria, we measured the $[Ca^{2+}]_m$ decline when extramitochondrial Ca^{2+} was removed (from 300 to 0 nM) with different $[Na^+]_c$ (varied from 0 to 50 mM) as a function of mitochondrial Ca^{2+} extrusion. Figure 6*A* demonstrates the Na^+-dependent declines in $[Ca^{2+}]_m$ under normal $\Delta\Psi_m$. The higher $[Na^+]_c$ caused faster declines in $[Ca^{2+}]_m$.

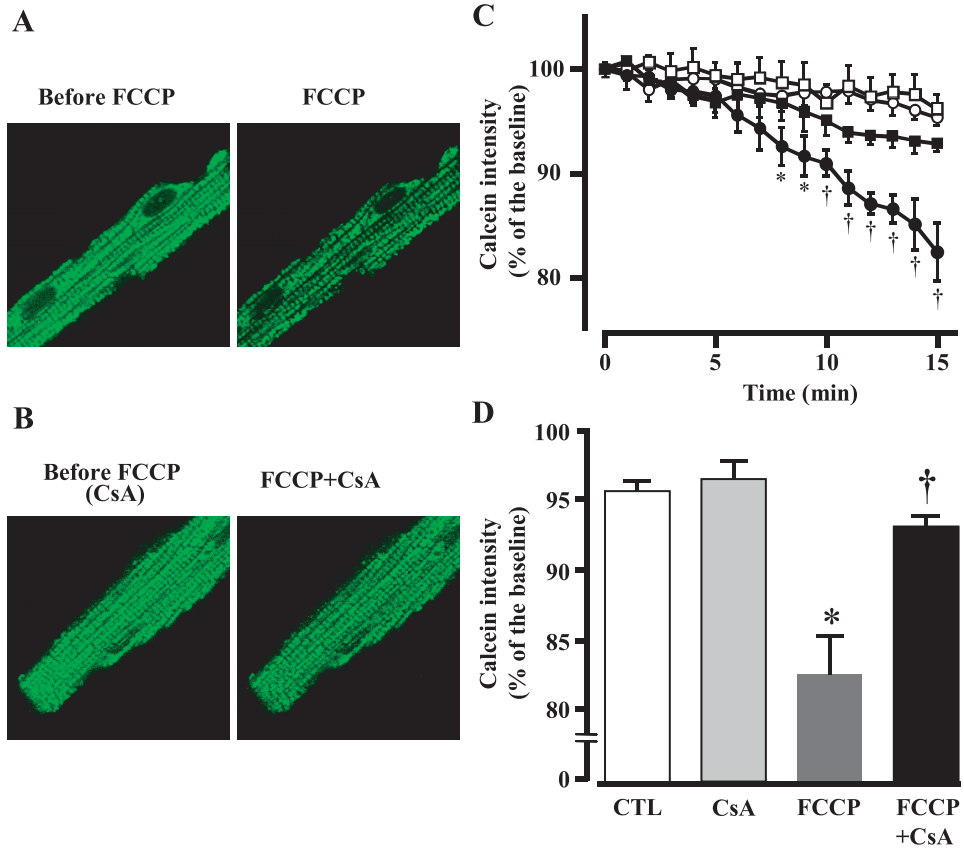

Fig. 4. Imaging of mitochondrial permeability transition pore (mPTP) opening with calcein in permeabilized myocytes. *A*: calcein images of permeabilized myocytes were obtained before and after 15-min FCCP perfusion (0.3 μM). *B*: after 5-min pretreatment with cyclosporin A (CsA, 0.1 μM; *left*), FCCP was applied in the presence of CsA (*right*). *C*: time courses of the changes in calcein signals during perfusion of a control internal solution (○, control, $[Ca^{2+}]_c$ = 300 nM), CsA (□, 0.1 μM), FCCP (●, 0.3 μM), and FCCP in the presence of CsA (■, FCCP + CsA). *$P < 0.05$ vs. control; †$P <$ 0.01 vs. control by ANOVA. *D*: calcein intensities after a 15-min perfusion of each solution were summarized. Data are presented as the percentage of baseline calcein signal (before perfusion). *$P < 0.01$ vs. control; †$P < 0.01$ vs. FCCP by ANOVA.

Downloaded from http://ajpheart.physiology.org/ by 10.220.33.5 on October 6, 2016

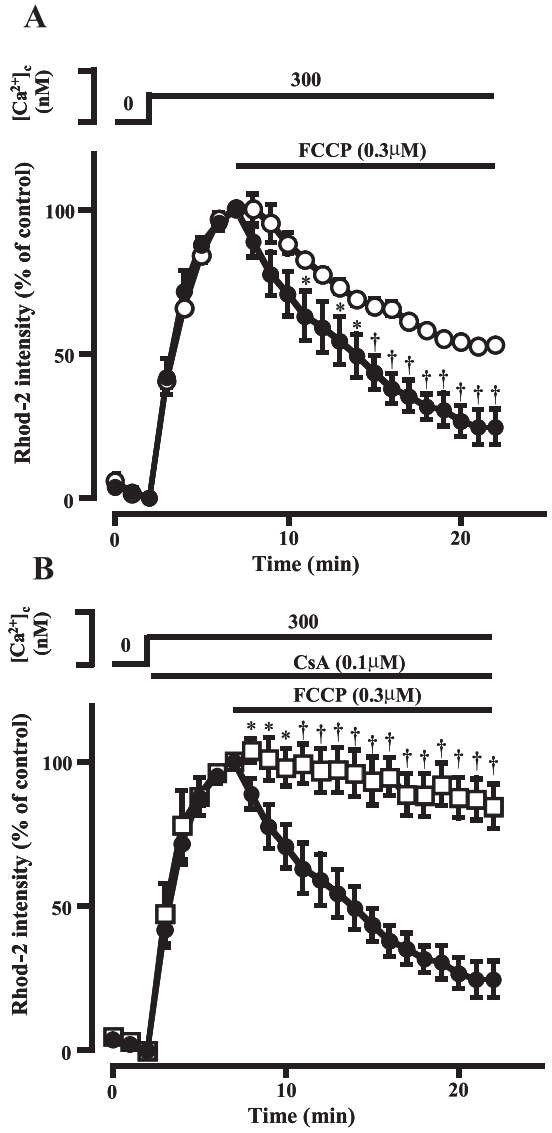

Fig. 5. Mitochondrial Ca^{2+} influx via the mPTP and Ca^{2+} efflux via mitochondrial Na^+/Ca^{2+} exchange (mitoNCX) under $\Delta\Psi_m$ dissipation. *A*: time courses of the changes in rhod-2 signals after perfusion of FCCP (0.3 μM) in the absence (○, $n = 4$) and presence (●, $n = 4$) of CsA (0.1 μM). In the CsA-pretreated myocytes, cells were exposed to CsA for 5 min and then FCCP was added to the internal solution ($[Ca^{2+}]_c = 300$ nM) in the presence of CsA. $^*P < 0.05$; $^\dagger P < 0.01$ vs. without CsA by ANOVA. *B*: time courses of changes in rhod-2 signals after perfusion of FCCP (0.3 μM). Myocytes were pretreated with CsA (0.1 μM) for 5 min and then FCCP was applied to a normal Na^+ {●, extramitochondrial Na^+ concentration ($[Na^+]_c$) = 10 mM} or a Na^+-free (□, $[Na^+]_c = 0$ mM) internal solution in the presence of CsA. $^*P < 0.05$; $^\dagger P < 0.01$ vs. $[Na^+]_c = 10$ mM by ANOVA.

Because the declines in $[Ca^{2+}]_m$ were slowed by the mitoNCX inhibitors diltiazem (100 μM; $n = 4$) and clonazepam (100 μM; data not shown) with 10 mM $[Na^+]_c$, it is likely that a Na^+-mediated Ca^{2+} efflux occurred via the mitoNCX. The value of $t_{1/2}$ (the time required for the rhod-2 signal to decrease to one-half of maximal amplitude) was used to evaluate the rate of $[Ca^{2+}]_m$ decline. Figure 6*B* shows that $[Na^+]_c$, which yields a half-maximal rate of decrease ($k_{0.5}$) for $[Ca^{2+}]_m$, was 3.6 mM with a Hill coefficient of 1.8 for the normal $\Delta\Psi_m$ condition. Figure 6*C* demonstrates the Na^+-dependent declines in $[Ca^{2+}]_m$ when $\Delta\Psi_m$ was dissipated by 0.3 μM FCCP. To eliminate the contribution of the mPTP, cells were pretreated with 0.1 μM CsA. Although the reduction in $[Ca^{2+}]_m$ was slowed during dissipated $\Delta\Psi_m$ compared with normal $\Delta\Psi_m$, mitochondria certainly extrude Ca^{2+} in a Na^+-dependent manner. The $k_{0.5}$ of $[Na^+]_c$ was 7.6 mM with a Hill coefficient of 1.7 during $\Delta\Psi_m$ dissipation (Fig. 6*D*).

DISCUSSION

In this study, we measured $[Ca^{2+}]_m$ in chemically skinned cardiac myocytes and investigated the regulation of $[Ca^{2+}]_m$ in both normal and dissipated $\Delta\Psi_m$. Our important experimental findings include the following: *1*) the mitochondrial Ca^{2+} uniporter accumulates Ca^{2+} in a $\Delta\Psi_m$-dependent manner in the physiological ranges of $[Ca^{2+}]_c$; *2*) $\Delta\Psi_m$ dissipation opens the mPTP and results in Ca^{2+} influx into mitochondria via the mPTP; and *3*) although $\Delta\Psi_m$ dissipation reduces mitoNCX activity, mitoNCX extrudes Ca^{2+} from the matrix even after $\Delta\Psi_m$ dissipation.

Measuring $[Ca^{2+}]_m$ using rhod-2 signals. Rhod-2-AM is used to measure mitochondrial Ca^{2+}, because rhod-2 itself has a net positive charge and is selectively loaded into mitochondria, which have a negative $\Delta\Psi_m$ (1, 35). However, when cells were simply loaded by the membrane-permeate AM-ester form, it was difficult to monitor the mitochondrial rhod-2 signal while avoiding signal contamination from the cytosolic dyes. To improve this problem, further ingenuities such as employing cold-warm loading (1), using dihydro-rhod-2 (35), or permeabilizing the sarcolemmal membrane (32) were required. In the present study, the following evidence allowed us to conclude that the rhod-2 signal in the permeabilized myocytes indeed represented $[Ca^{2+}]_m$: *1*) rhod-2 signal distribution in a permeabilized myocyte showed complete overlap with Mito Tracker Green (see Fig. 1*A*); *2*) rhod-2 intensity increased in response to $[Ca^{2+}]_c$ (see Fig. 1, *B* and *C*); and *3*) rhod-2 intensity did not increase when the Ca^{2+} uniporter was inhibited by RuR or FCCP (see Fig. 2, *B–D*).

Even in permeabilized myocytes, rhod-2 fluorescence could distribute to the sarcoplasmic reticulum (SR), and thus the changes in rhod-2 signals in permeabilized myocytes might be contaminated by SR Ca^{2+}. To eliminate this possibility, we repeated our $[Ca^{2+}]_m$ studies in the presence of thapsigargin (5 μM), which is an inhibitor of SR Ca^{2+}-ATPase. The results were quite similar to those obtained without thapsigargin (data not shown). Thus we determined that the contribution of the SR Ca^{2+} concentration was negligible in our experimental conditions.

Mitochondrial Ca^{2+} uptake via the Ca^{2+} uniporter. Although mitochondria could accumulate a significant amount of Ca^{2+} from the cytosol during intracellular Ca^{2+} signaling, previous studies that used isolated mitochondria indicated a very low affinity of the mitochondrial Ca^{2+} uniporter for Ca^{2+}, that is, an apparent K_m of 4.7–10 μM (3, 4, 16). Recently, Kirichok et al. (21) showed an extremely high Ca^{2+} affinity ($K_m \leq 2$ nM) and a high Ca^{2+} selectivity of the mitochondrial Ca^{2+} uniporter by patch-clamping the inner mitochondrial membrane of mitoplasts. Here we have shown that mitochondrial Ca^{2+} influx via the Ca^{2+} uniporter occurred even in the physiological $[Ca^{2+}]_c$ range, where the bulk $[Ca^{2+}]_c$ was 177–600 nM.

Downloaded from http://ajpheart.physiology.org/ by 10.220.33.5 on October 6, 2016

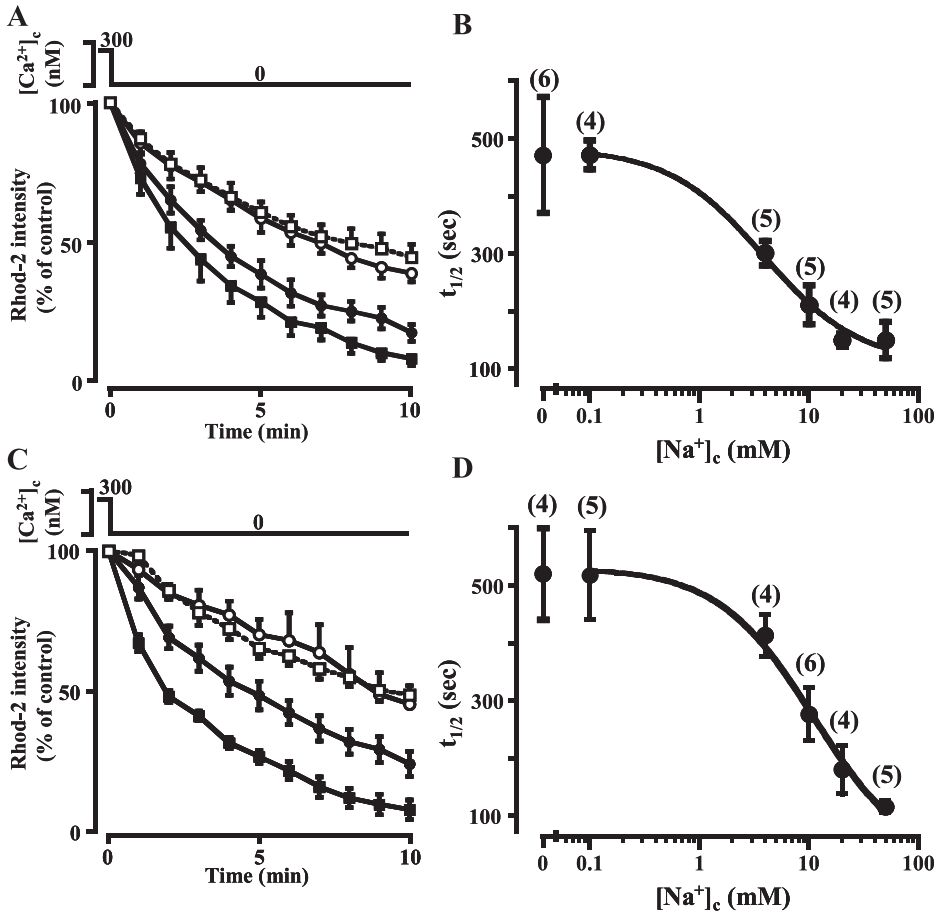

Fig. 6. Effects of $\Delta\Psi_m$ on the Na^+-dependent mitochondrial Ca^{2+} extrusion. *A* and *C*: Na^+-dependent mitochondrial Ca^{2+} extrusion in normal (*A*) and dissipated (*C*) $\Delta\Psi_m$ are shown. Extramitochondrial Ca^{2+} was removed (300 to 0 nM) in the presence of different $[Na^+]_c$ (○, 0 mM; ●, 10 mM; ■, 50 mM) or in the presence of diltiazem (□, 100 μM) with normal $[Na^+]_c$ (10 mM), and the decays of $[Ca^{2+}]_m$ were monitored. Myocytes were exposed to CsA for 5 min to exclude the contribution of the mPTP, and then FCCP was added to the internal solution ($[Ca^{2+}]_c$ = 0 nM) in the presence of CsA (*C*). *B* and *D*: time required for $[Ca^{2+}]_m$ to decrease to one-half maximum ($t_{1/2}$) was used to analyze the rates of mitochondrial Ca^{2+} extrusion at varied $[Na^+]_c$ (0, 0.1, 4, 10, 20, and 50 mM). Each point indicates a mean ± SE. Data were fitted by a Hill equation with $k_{0.5}$ = 3.6 mM and a Hill coefficient of 1.8 in the normal $\Delta\Psi_m$ (*B*), and with $k_{0.5}$ = 7.6 mM and a Hill coefficient of 1.7 in the dissipated $\Delta\Psi_m$ (*D*). Numbers of cells are in parentheses.

In this study, $[Ca^{2+}]_m$ decreased in response to the changes in partially depolarized $\Delta\Psi_m$ (see Fig. 3*B*). These results are in good correspondence with those obtained from isolated mitochondria (10, 11). Because Ca^{2+} entry into the mitochondria directly reflects the activity of the Ca^{2+} uniporter (see Fig. 2, *B–D*), and Ca^{2+} efflux from mitochondria by mitoNCX is not accelerated by $\Delta\Psi_m$ depolarization (see Fig. 6), the reduction in $[Ca^{2+}]_m$ could be due to the decreased driving force for the Ca^{2+} uniporter by the $\Delta\Psi_m$ depolarization. In contrast, when $\Delta\Psi_m$ was completely dissipated, $[Ca^{2+}]_m$ remained at one-half of the control level (see Fig. 3*C*). Because $[Ca^{2+}]_m$ did not increase after pretreatment with 0.3 μM FCCP in our experimental procedures (see Fig. 2*C*), Ca^{2+} influx via the Ca^{2+} uniporter was inhibited after dissipation of the $\Delta\Psi_m$. These results indicate that pathways other than the Ca^{2+} uniporter might be involved in regulation of $[Ca^{2+}]_m$. Montero et al. (28) have demonstrated that when $\Delta\Psi_m$ was depolarized, the action of the Ca^{2+} uniporter was reversed, and Ca^{2+} could be released via the Ca^{2+} uniporter. However, the simultaneous application of 0.3 μM FCCP plus 1 μM RuR did not alter $[Ca^{2+}]_m$ in our experiments (data not shown), which indicates that there is little contribution of the Ca^{2+} uniporter to $[Ca^{2+}]_m$ regulation after $\Delta\Psi_m$ dissipation.

Dissipation of $\Delta\Psi_m$, opening of mPTP, and $[Ca^{2+}]_m$. The mPTP opening and closing are strictly regulated by multiple factors such as reactive oxygen radicals, matrix pH, $[Ca^{2+}]_m$, and $\Delta\Psi_m$ (8, 12, 13, 24). It has also been reported (4, 10, 11) that the mPTP serves as a mitochondrial Ca^{2+} flux pathway during pathophysiological conditions. Earlier we reported (20) a method for assessing mPTP opening by monitoring mitochondrial calcein signals whereby cells were loaded with calcein-AM, and cytosolic fluorescence was quenched with Co^{2+}. Here we advanced this method using permeabilized myocytes and showed that the complete dissipation of $\Delta\Psi_m$ accelerated calcein leakage from mitochondria in a CsA-sensitive manner (see Fig. 4). To confirm that there is calcein leakage when mitochondrial permeability is altered, we tested the effects of the pore-forming antibiotic alamethicin (3 μM) on changes in calcein signals. As was found by Petronilli et al. (30), alamethicin-induced pore formation caused abrupt and complete loss of calcein fluorescence from the matrix within 5 min (data not shown). Because CsA is a well-known inhibitor of the mPTP (8, 12, 13, 24), it is suggested that the mPTP opened when $\Delta\Psi_m$ was completely dissipated by FCCP. Importantly, the calcein leakage from mitochondria by FCCP was almost abolished in the Ca^{2+}-free solution (data not shown), which indicates that the opening of the mPTP strongly depends on matrix Ca^{2+}. We also showed that the application of CsA alone did not alter calcein leakage (see Fig. 4, *C* and *D*), which indicates that mPTP opening is not significant in energized (fully polarized) mitochondria. Although the Ca^{2+}-activated protein phosphatase calcineurin is also inhibited by CsA, the effect of CsA on calcineurin might be negligible, because the sarcolemmal membrane was permeabilized, and cytosolic signal proteins were released in our experiments.

Downloaded from http://ajpheart.physiology.org/ by 10.220.33.5 on October 6, 2016

The opening of the mPTP was originally described (14, 17) in isolated mitochondria as a massive mitochondrial swelling under the conditions of matrix Ca^{2+} overload, oxidative stress, and depleted adenine nucleotide contents. In those studies, an extremely high concentration of extramitochondrial Ca^{2+} was administrated that caused mitochondrial Ca^{2+} release as a result of mPTP opening, with an apparent K_m of 16 μM at pH 7.0 (14). In this study, we showed that there was an mPTP-related Ca^{2+} influx into mitochondria after the $\Delta\Psi_m$ dissipation (see Fig. 5*A*). Because the opening of the mPTP allows nonselective ion permeability (8, 12, 13, 24), whether Ca^{2+} would be extruded from mitochondria or loaded into mitochondria might depend on the Ca^{2+} concentration gradient between the cytosol and matrix. Miyata et al. (26) reported that in rat myocytes, the gradient between $[Ca^{2+}]_m$ and $[Ca^{2+}]_c$ is less than unity at $[Ca^{2+}]_c < 500$ nM but rapidly increases at values of $[Ca^{2+}]_c$ higher than 500 nM. Monteith and Blaustein (27) also reported that $[Ca^{2+}]_m$ did not increase above $[Ca^{2+}]_c$ when serotonin administration (10 μM) elevated $[Ca^{2+}]_c$ to 350 nM. In our preliminary experiments, application of the Ca^{2+} ionophore ionomycin (10 μM) to the Ca^{2+}-loaded mitochondria ($[Ca^{2+}]_c = 300$ nM) increased the rhod-2 intensity (data not shown). Thus the Ca^{2+} gradient between the cytosol and mitochondria ($[Ca^{2+}]_m < [Ca^{2+}]_c$) in our experimental conditions might have caused a Ca^{2+} influx into mitochondria when the mPTP opened. However, it should be noted that the nonselective pores could leak the fluorescence probe from the mitochondria, and this could lead to underestimation of the $[Ca^{2+}]_m$ measurement when the mPTP was opened by FCCP.

Na^+/Ca^{2+} exchange and $[Ca^{2+}]_m$. We have demonstrated that decays in $[Ca^{2+}]_m$ were dependent on $[Na^+]_c$ under conditions of both normal and dissipated $\Delta\Psi_m$, which suggests that mitoNCX plays a dominant role in mitochondrial Ca^{2+} efflux pathways in cardiac myocytes (see Fig. 6, *A* and *C*). The $[Na^+]_c$ that achieved a half-maximal $[Ca^{2+}]_m$ extrusion rate via mitoNCX was 3.6 mM (see Fig. 6*B*) under normal $\Delta\Psi_m$ and 7.6 mM (see Fig. 6*D*) under the condition of $\Delta\Psi_m$ dissipation. This is in good agreement with previous studies, which reported that the half-maximal rate of Ca^{2+} efflux by mitoNCX was 2.6 mM in endothelial cells (32) and 4.4 mM in cardiac myocytes (7) under normal $\Delta\Psi_m$. Although many studies have proposed that the exchange rate of Na^+ and Ca^{2+} in mitoNCX is 2:1 (25), Jung et al. (19) reported that the Na^+-to-Ca^{2+} ratio in mitoNCX could be altered. Moreover, Griffiths (9) demonstrated the reversal of mitoNCX under $\Delta\Psi_m$ collapse in isolated myocytes. However, in the present study, we showed that mitoNCX indeed extruded Ca^{2+} from the matrix even under the condition of $\Delta\Psi_m$ dissipation (see Figs. 5*B* and 6). Our results have several significances regarding regulation of $[Ca^{2+}]_m$. First, under physiological conditions (where $[Na^+]_c = \sim 10$ mM and $\Delta\Psi_m$ is fully polarized), the mitochondrial Ca^{2+} extrusion rate by mitoNCX is already in a nearly maximal state. Second, in a condition of $\Delta\Psi_m$ dissipation such as ischemia, although the activity rate of mitoNCX was impaired, mitoNCX extruded Ca^{2+} from the matrix and there was no Ca^{2+} influx into the mitochondria by the reversal mode of mitoNCX. Third, in the situation of reperfusion where $[Na^+]_c$ and $[Ca^{2+}]_c$ significantly elevate and there is a recovery of $\Delta\Psi_m$ (2, 31), the activity of mitoNCX might not be accelerated so much as it conquers excessive mitochondrial Ca^{2+} overload (because the activity of mitoNCX is nearly saturated at the physiological range of $[Na^+]_c$). These findings could provide additional understanding of the mechanisms of mitochondrial damage during ischemia-reperfusion.

We conclude that in skinned rat ventricular myocytes, *1*) the mitochondrial Ca^{2+} uniporter accumulates Ca^{2+} in a $\Delta\Psi_m$-dependent manner within the physiological ranges of $[Ca^{2+}]_c$, *2*) the dissipation of $\Delta\Psi_m$ opens the mPTP and results in Ca^{2+} influx into the mitochondria via the mPTP, and *3*) although the activity of mitoNCX is impaired when $\Delta\Psi_m$ is dissipated, mitoNCX extrudes Ca^{2+} from the matrix even after $\Delta\Psi_m$ dissipation. Our findings underscore the basic understanding of mitochondrial Ca^{2+} regulation within pathophysiological conditions such as ischemia-reperfusion injury. Additional studies are required to elucidate the roles of mitoNCX and mPTP opening within the mechanisms of ischemia-reperfusion injury.

GRANTS

This work was supported by Japan Grants-in-Aid 13670703 (to H. Katoh) and 50135258 (to H. Hayashi) and by a grant-in-aid from the Center of Excellence from the Ministry of Education, Culture, Sports, Science, and Technology.

REFERENCES

1. **Akao M, O'Rourke B, Teshima Y, Seharaseyon J, and Marban E.** Mechanistically distinct steps in the mitochondrial death pathway triggered by oxidative stress in cardiac myocytes. *Circ Res* 92: 186–194, 2003.
2. **Allen DG and Xiao XH.** Role of the cardiac Na^+/H^+ exchanger during ischemia and reperfusion. *Cardiovasc Res* 57: 934–941, 2003.
3. **Bassani RA, Fagian MM, Bassani JW, and Vercesi AE.** Changes in calcium uptake rate by rat cardiac mitochondria during postnatal development. *J Mol Cell Cardiol* 30: 2013–2023, 1998.
4. **Bernardi P.** Mitochondrial transport of cations: channels, exchangers, and permeability transition. *Physiol Rev* 79: 1127–1155, 1999.
5. **Bernardi P, Veronese P, and Petronilli V.** Modulation of the mitochondrial cyclosporin A-sensitive permeability transition pore. I. Evidence for two separate Mg^{2+} binding sites with opposing effects on the pore open probability. *J Biol Chem* 268: 1005–1010, 1993.
6. **Brierley GP, Baysal K, and Jung DW.** Cation transport systems in mitochondria: Na^+ and K^+ uniporters and exchangers. *J Bioenerg Biomembr* 26: 519–526, 1994.
7. **Cox DA and Matlib MA.** A role for the mitochondrial Na^+-Ca^{2+} exchanger in the regulation of oxidative phosphorylation in isolated heart mitochondria. *J Biol Chem* 268: 938–947, 1993.
8. **Crompton M.** The mitochondrial permeability transition pore and its role in cell death. *Biochem J* 341: 233–249, 1999.
9. **Griffiths EJ.** Reversal of mitochondrial Na/Ca exchange during metabolic inhibition in rat cardiomyocytes. *FEBS Lett* 453: 400–404, 1999.
10. **Gunter TE, Buntinas L, Sparagna G, Eliseev R, and Gunter K.** Mitochondrial calcium transport: mechanisms and functions. *Cell Calcium* 28: 285–296, 2000.
11. **Gunter TE, Gunter KK, Sheu SS, and Gavin CE.** Mitochondrial calcium transport: physiological and pathological relevance. *Am J Physiol Cell Physiol* 267: C313–C339, 1994.
12. **Halestrap AP.** The mitochondrial permeability transition: its molecular mechanism and role in reperfusion injury. *Biochem Soc Symp* 66: 181–203, 1999.
13. **Halestrap AP, McStay GP, and Clarke SJ.** The permeability transition pore complex: another view. *Biochimie* 84: 153–166, 2002.
14. **Haworth RA and Hunter DR.** The Ca^{2+}-induced membrane transition in mitochondria. II. Nature of the Ca^{2+} trigger site. *Arch Biochem Biophys* 195: 460–467, 1979.
15. **Hayashi H, Miyata H, Noda N, Kobayashi A, Hirano M, Kawai T, and Yamazaki N.** Intracellular Ca^{2+} concentration and pH_i during metabolic inhibition. *Am J Physiol Cell Physiol* 262: C628–C634, 1992.
16. **Heaton GM and Nicholls DG.** The calcium conductance of the inner membrane of rat liver mitochondria and the determination of the calcium electrochemical gradient. *Biochem J* 156: 635–646, 1976.

Downloaded from http://ajpheart.physiology.org/ by 10.220.33.5 on October 6, 2016

17. **Hunter DR, Haworth RA, and Southard JH.** Relationship between configuration, function, and permeability in calcium-treated mitochondria. *J Biol Chem* 251: 5069–5077, 1976.
18. **Ichas F and Mazat JP.** From calcium signaling to cell death: two conformations for the mitochondrial permeability transition pore. Switching from low- to high-conductance state. *Biochim Biophys Acta* 1366: 33–50, 1998.
19. **Jung DW, Baysal K, and Brierley GP.** The sodium-calcium antiport of heart mitochondria is not electroneutral. *J Biol Chem* 270: 672–678, 1995.
20. **Katoh H, Nishigaki N, and Hayashi H.** Diazoxide opens the mitochondrial permeability transition pore and alters Ca^{2+} transients in rat ventricular myocytes. *Circulation* 105: 2666–2671, 2002.
21. **Kirichok Y, Krapivinsky G, and Clapham DE.** The mitochondrial calcium uniporter is a highly selective ion channel. *Nature* 427: 360–364, 2004.
22. **Korge P, Honda HM, and Weiss JN.** Protection of cardiac mitochondria by diazoxide and protein kinase C: implications for ischemic preconditioning. *Proc Natl Acad Sci USA* 99: 3312–3317, 2002.
23. **Korge P, Honda HM, and Weiss JN.** Regulation of the mitochondrial permeability transition by matrix Ca^{2+} and voltage during anoxia/reoxygenation. *Am J Physiol Cell Physiol* 280: C517–C526, 2001.
24. **Lemasters JJ, Nieminen AL, Qian T, Trost LC, Elmore SP, Nishimura Y, Crowe RA, Cascio WE, Bradham CA, Brenner DA, and Herman B.** The mitochondrial permeability transition in cell death: a common mechanism in necrosis, apoptosis and autophagy. *Biochim Biophys Acta* 1366: 177–196, 1998.
25. **Li W, Shariat-Madar Z, Powers M, Sun X, Lane RD, and Garlid KD.** Reconstitution, identification, purification, and immunological characterization of the 110-kDa Na^+/Ca^{2+} antiporter from beef heart mitochondria. *J Biol Chem* 267: 17983–17989, 1992.
26. **Miyata H, Silverman HS, Sollott SJ, Lakatta EG, Stern MD, and Hansford RG.** Measurement of mitochondrial free Ca^{2+} concentration in living single rat cardiac myocytes. *Am J Physiol Heart Circ Physiol* 261: H1123–H1134, 1991.
27. **Monteith GR and Blaustein MP.** Heterogeneity of mitochondrial matrix free Ca^{2+}: resolution of Ca^{2+} dynamics in individual mitochondria in situ. *Am J Physiol Cell Physiol* 276: C1193–C1204, 1999.
28. **Montero M, Alonso MT, Albillos A, Garcia-Sancho J, and Alvarez J.** Mitochondrial Ca^{2+}-induced Ca^{2+} release mediated by the Ca^{2+} uniporter. *Mol Biol Cell* 12: 63–71, 2001.
29. **Nomura N, Satoh H, Terada H, Matsunaga M, Watanabe H, and Hayashi H.** CaMKII-dependent reactivation of SR Ca^{2+} uptake and contractile recovery during intracellular acidosis. *Am J Physiol Heart Circ Physiol* 283: H193–H203, 2002.
30. **Petronilli V, Miotto G, Canton M, Brini M, Colonna R, Bernardi P, and Di Lisa F.** Transient and long-lasting openings of the mitochondrial permeability transition pore can be monitored directly in intact cells by changes in mitochondrial calcein fluorescence. *Biophys J* 76: 725–734, 1999.
31. **Satoh H, Hayashi H, Katoh H, Terada H, and Kobayashi A.** Na^+/H^+ and Na^+/Ca^{2+} exchange in regulation of $[Na^+]_i$ and $[Ca^{2+}]_i$ during metabolic inhibition. *Am J Physiol Heart Circ Physiol* 268: H1239–H1248, 1995.
32. **Sedova M and Blatter LA.** Intracellular sodium modulates mitochondrial calcium signaling in vascular endothelial cells. *J Biol Chem* 275: 35402–35407, 2000.
33. **Suleiman MS, Halestrap AP, and Griffiths EJ.** Mitochondria: a target for myocardial protection. *Pharmacol Ther* 89: 29–46, 2001.
34. **Weiss JN, Korge P, Honda HM, and Ping P.** Role of the mitochondrial permeability transition in myocardial disease. *Circ Res* 93: 292–301, 2003.
35. **Williams DA, Bowser DN, and Petrou S.** Confocal Ca^{2+} imaging of organelles, cells, tissues, and organs. *Methods Enzymol* 307: 441–469, 1999.

Downloaded from http://ajpheart.physiology.org/ by 10.220.33.5 on October 6, 2016